Revisiting the annihilation corrections in nonleptonic $\bar{B}_s^0$ decays within QCD factorization

Qin Chang,[1,2,*] Xiao-Wei Cui,[1] Lin Han,[2] and Ya-Dong Yang[2,3,†]

[1]*Department of Physics, Henan Normal University, Xinxiang, Henan 453007, People's Republic of China*
[2]*Institute of Particle Physics, Huazhong Normal University, Wuhan, Hubei 430079, People's Republic of China*
[3]*Key Laboratory of Quark and Lepton Physics, Ministry of Education, People's Republic of China*

(Received 22 July 2012; published 19 September 2012)

Motivated by the recent measurements of nonleptonic $\bar{B}_s^0$ decays by the CDF and LHCb collaborations, especially the large $\mathcal{B}(\bar{B}_s^0 \to \pi^+\pi^-)$, we revisit the hard spectator and annihilation corrections in $\bar{B}_s^0$ decays within a QCD factorization approach, with two schemes for the possible parameters for the known end-point divergence appearing in the estimation of the hard spectator and annihilation diagrams. The first one is to conservatively estimate the possible contributions by parametrization (scheme I); another one uses an infrared finite gluon propagator (scheme II) to regulate the end-point singularity. In scheme I, with the constraints from the measured $\bar{B}_s^0 \to PP(VV)$ decays, two (four) restricted solutions of the parameter spaces are found. In scheme II, we find that most of the theoretical predictions agree well with the experimental data with a single parameter $m_g \sim 0.5$ GeV. However, within both schemes, $\mathcal{B}(\bar{B}_s^0 \to \phi\phi)$ are always much larger than $\mathcal{B}(\bar{B}_s^0 \to K^{*0}\bar{K}^{*0})$, in contrast to the experimental results $\mathcal{B}(\bar{B}_s^0 \to \phi\phi) \simeq \mathcal{B}(\bar{B}_s^0 \to K^{*0}\bar{K}^{*0})$. It is noted that the pattern $\mathcal{B}(\bar{B}_s^0 \to \phi\phi) > \mathcal{B}(\bar{B}_s^0 \to K^{*0}\bar{K}^{*0})$ also persists in other theoretical frameworks; thus, the present experimental result $\mathcal{B}(\bar{B}_s^0 \to \phi\phi) \simeq \mathcal{B}(\bar{B}_s^0 \to K^{*0}\bar{K}^{*0})$ raises a challenge to theoretical approaches for B nonleptonic decays. Further refined measurements and theoretical studies are called for to resolve such a possible anomaly.

DOI: 10.1103/PhysRevD.86.054016 PACS numbers: 13.25.Hw, 11.30.Hv, 12.38.Bx

I. INTRODUCTION

The pure annihilation nonleptonic B meson decays, without the interference induced by spectator diagrams, are very suitable for probing the strength of annihilation contribution and exploiting the related mechanism. Recently, the CDF and LHCb collaborations have reported the evidence of the pure annihilation decay $\bar{B}_s^0 \to \pi^+\pi^-$, with a significance of 3.7σ and 5.3σ, respectively [1,2],

$$\mathcal{B}(\bar{B}_s^0 \to \pi^+\pi^-) = (0.57 \pm 0.15(\text{stat}) \pm 0.10(\text{syst})) \times 10^{-6} \quad \text{CDF}, \tag{1}$$

$$\mathcal{B}(\bar{B}_s^0 \to \pi^+\pi^-) = (0.98^{+0.23}_{-0.19}(\text{stat}) \pm 0.11(\text{syst})) \times 10^{-6} \quad \text{LHCb}, \tag{2}$$

as well as the branching fraction of the pure annihilation decay $\bar{B}_d^0 \to K^+K^-$, [1,2]

$$\mathcal{B}(\bar{B}_d^0 \to K^+K^-) = (0.23 \pm 0.10(\text{stat}) \pm 0.10(\text{syst})) \times 10^{-6} \quad \text{CDF}, \tag{3}$$

$$\mathcal{B}(\bar{B}_d^0 \to K^+K^-) = (0.13^{+0.06}_{-0.05}(\text{stat}) \pm 0.07(\text{syst})) \times 10^{-6} \quad \text{LHCb}. \tag{4}$$

Averaging the experimental data in Eqs. (1) and (2), the heavy flavor averaging group (HFAG) gives [3]

$$\mathcal{B}(\bar{B}_s^0 \to \pi^+\pi^-) = (0.73 \pm 0.14) \times 10^{-6} \quad \text{HFAG}. \tag{5}$$

Roughly averaging the experimental data in Eqs. (3) and (4), we get

$$\mathcal{B}(\bar{B}_d^0 \to K^+K^-) = (0.16 \pm 0.08) \times 10^{-6}. \tag{6}$$

Theoretically, the pure annihilation nonleptonic B meson decays are expected to be much more rare with a branching fraction at the level 10^{-7} or less, due to the fact that the annihilation corrections are formally Λ_{QCD}/m_b power suppressed. Together with the chirally enhanced power corrections, they offer interesting probes for the dynamical mechanism governing these decays and exploration of (CP) violations, and therefore have attracted much more attention recently [4–7]. Unfortunately, in the collinear factorization approach, the calculation of annihilation corrections always suffers from end-point divergence. Within the perturbative QCD (pQCD) approach [8], such divergence is regulated by introducing the parton transverse momentum k_T at the expense of modeling additional k_T dependence of meson distribution functions, and presents large, complex annihilation corrections [6,8]. The most recently renewed pQCD estimations of $\mathcal{B}(\bar{B}_s^0 \to \pi^+\pi^-)$ and $\mathcal{B}(\bar{B}_d^0 \to K^+K^-)$ [7] are in good agreement with the CDF and LHCb measurements; however, a systematic examination combined with other correlated decays in the same framework is not available yet. In the soft-collinear effective theory (SCET) [9], the annihilation diagrams are factorable and real [10] to the leading power of $\mathcal{O}(\alpha_s(m_b)\Lambda_{\text{QCD}}/m_b)$.

*changqin@htu.cn
†yangyd@iopp.ccnu.edu.cn

In the QCD factorization approach (QCDF) [11], there are two main ways to deal with the end-point singularity in a weak annihilation calculation: (i) scheme I, parametrization in a model-independent way [12] with at least two phenomenological parameters introduced, for example, $X_A = \int_0^1 dy/y = \ln(m_b/\Lambda_h)(1 + \rho_A e^{i\phi_A})$; (ii) scheme II, using the infrared finite gluon propagator [13,14], for example, $1/k^2 \to 1/(k^2 - M_g(k^2) + i\epsilon)$.

As a popular method, scheme I is widely used in the theoretical calculations [12,15–17]. Fitting to the data of $B_{u,d} \to PP$ decays, a favored parameter value choice "Scenario S4" is obtained in Ref. [12]: $\rho_A^{u,d}(PP) \sim 1$ and $\phi_A^{u,d}(PP) \sim -55°$, which leads to the prediction

$$\mathcal{B}(\bar{B}_d^0 \to K^+K^-) = 0.070 \times 10^{-6}. \tag{7}$$

Assuming the default values of $\rho_A(PP)$ and $\phi_A(PP)$ in B_s decays are similar to that in $B_{u,d}$ decays, Cheng *et al.* give the prediction [17]

$$\mathcal{B}(\bar{B}_s^0 \to \pi^+\pi^-) = (0.26^{+0.00+0.10}_{-0.00-0.09}) \times 10^{-6}. \tag{8}$$

It has been noted that the above QCDF predictions are significantly smaller than the measurements in Eqs. (5) and (6). In particular, the default value $\mathcal{B}(\bar{B}_s^0 \to \pi^+\pi^-) = 0.26 \times 10^{-6}$ is about 3.4σ lower than the experimental data $(0.73 \pm 0.14) \times 10^{-6}$, which implies much larger possible annihilation contributions in B_s decays than previously expected. Using the CDF results in Eq. (1) solely, a detailed study about this topic has been performed by Zhu [4]. Assuming universal values of $\rho_A(PP)$ and $\phi_A(PP)$ for B_d and B_s decays, it is found that the results of QCDF are hardly in agreement with all of the well-measured $B \to PP$ decays. Then, if the recent measurement of LHCb in Eq. (2) is considered, the tension would be further enlarged, which may imply the parameters ρ_A and ϕ_A are nonuniversal in B_d and B_s decays. So, it is worthwhile to fit their values with available data of B_d and B_s decays, respectively, and update the QCDF predictions.

Within scheme II, the formula for annihilation corrections for $B \to PP$ and PV decays have been given in Ref. [14]. In this scheme, with the only one input parameter effective gluon mass scale $m_g = 0.50 \pm 0.05$ GeV, the theoretical predictions of the observables for $B_{u,d} \to \pi K$, ρK and πK^* decays are consistent with the experimental data [14]. So, it is a good idea to check if its predictions for the pure annihilation decays are in agreement with the same effective gluon mass scale parameter. Furthermore, the pure annihilation $B_{d,s} \to VV$ decays, which involve more observables, may play an important role in testing the methods of the end-point singularity regulation. So, in this paper, we calculate the annihilation corrections related to $B_{d,s} \to VV$ decays with the infrared finite gluon propagator.

In Sec. II, we briefly review the annihilation contributions within QCDF. In Secs. III and IV, with schemes I and II for the end-point divergence regulation, we revisit $\bar{B}_s^0 \to PP$, PV, and VV decay modes, respectively. In our evaluations, the pure annihilation B_s nonleptonic decays and the related well-measured ones are examined simultaneously. Section V contains our conclusions. Some amplitudes of $\bar{B}_s^0$ decays and the theoretical input parameters are summarized in Appendices A and B, respectively.

II. BRIEF REVIEW OF THE ANNIHILATION CORRECTIONS WITHIN QCDF

In the Standard Model (SM), the effective weak Hamiltonian responsible for $b \to p$ transitions is given as [18]

$$\mathcal{H}_{\rm eff} = \frac{G_F}{\sqrt{2}}\Big[V_{ub}V_{up}^*(C_1O_1^u + C_2O_2^u) + V_{cb}V_{cp}^*(C_1O_1^c + C_2O_2^c) - V_{tb}V_{tp}^*\Big(\sum_{i=3}^{10} C_iO_i + C_{7\gamma}O_{7\gamma} + C_{8g}O_{8g}\Big)\Big] + \text{H.c.}, \tag{9}$$

where $V_{qb}V_{qs}^*$ ($q = u$, c, and t) are products of the Cabibbo-Kobayashi-Maskawa (CKM) matrix elements, C_i the Wilson coefficients, and O_i the relevant four-quark operators.

With the effective weak Hamiltonian Eq. (9), the QCDF has been fully developed and extensively employed to calculate the hadronic B meson decays. The basic theoretical framework of $B_{u,d,s} \to PP$, PV, and VV decays can be found in Refs. [11,12,15–17]. In this paper, we adopt the same convention and formula given in Refs. [12,15], except for some corrections pointed out by Ref. [19]. It is noted that the strength and associated strong-interaction phase of annihilation corrections and hard spectator scattering contributions are numerically important to evaluate the branching ratios, the CP asymmetry, and the polarization observables. Unfortunately, such power correction terms always suffer from the end-point divergences, which violate the factorization. To probe their possible effects conservatively, the end-point divergent integrals are treated as signs of infrared sensitive contribution and usually parametrized by [12,15]:

$$\int_0^1 \frac{dx}{x} \to X_A, \qquad \int_0^1 dx \frac{\ln x}{x} \to -\frac{1}{2}(X_A)^2, \qquad \int_0^1 \frac{dx}{x^2} \to X_L, \tag{10}$$

where

$$X_A = (1 + \rho e^{i\phi}) \ln \frac{m_B}{\Lambda_h}, \qquad X_L = (1 + \rho e^{i\phi}) \frac{m_B}{\Lambda_h}, \tag{11}$$

with Λ_h being a typical scale of order 0.5 GeV, and ρ, ϕ being unknown real parameters. X_H is treated in the same manner. The different choices of the parameter spaces of ρ and ϕ correspond to various scenarios, which have been thoroughly discussed in Refs. [12,15–17].

Fitting the fruitful experimental measurements of $B_{u,d} \to PP$, PV, and VP decays, the favored scenarios

S4 are obtained in Ref. [12]. Furthermore, the fitted ρ and ϕ for $B_{u,d} \to VV$ decays are also given in Refs. [15,16]. Their results are summarized as

$$\rho_d^{PP} = 1, \qquad \phi_d^{PP} = -55°; \tag{12}$$

$$\rho_d^{PV} = 1, \qquad \phi_d^{PV} = -20°, \qquad \rho_d^{VP} = 1, \qquad \phi_d^{VP} = -70°; \tag{13}$$

$$\rho_d^{\rho K^*, K^* \bar{K}^*} = 0.78, \qquad \phi_d^{\rho K^*, K^* \bar{K}^*} = -43°;$$
$$\rho_d^{\phi K^*, K^* \omega} = 0.65, \qquad \phi_d^{\phi K^*, K^* \omega} = -53°. \tag{14}$$

Assuming the default values of ρ_A and ϕ_A in the B_s decays are similar to that in $B_{u,d}$ decays, Ref. [17] takes the values

$$\rho_s^{PP} = 1, \qquad \phi_s^{PP} = -55°; \tag{15}$$

$$\rho_s^{PV} = 0.85, \qquad \phi_s^{PV} = -30°,$$
$$\rho_s^{VP} = 0.9, \qquad \phi_s^{VP} = -65°; \tag{16}$$

$$\rho_s^{VV} = 0.70, \qquad \phi_s^{VV} = -55°, \tag{17}$$

as the inputs for the B_s decays. In this paper, we denote the above parameter space as "scenarios $\overline{S4}$" for convenience. It is noted that some nonleptonic $\bar{B}_s^0$ decays have been well measured in recent years, such as $\bar{B}_s^0 \to \pi^+\pi^-$, $\pi^- K^+$, $K^- K^+$, $K^{*0}\bar{K}^{*0}$, and $\phi\phi$ decays. So, it is worthwhile to check the above parameter values and refit them with the updated data of B_s decays. Furthermore, without the interference induced by spectator diagrams, the pure annihilation nonleptonic B_s meson decays, such as $\bar{B}_s^0 \to \pi\pi$, $\rho\pi$, and $\rho\rho$ decays, are very suitable for probing the strength of the annihilation corrections and related mechanism. So, in this paper, we mainly pay attention to these two types of B_s decays.

III. $\bar{B}_s^0 \to PP$ AND PV DECAY MODES

A. Within scheme I

With the annihilation parameters of scenarios $\overline{S4}$ for $\bar{B}_s^0 \to PP$ and PV decays given by Eqs. (15) and (16), and the other input parameters listed in Appendix B, the predictions for the observables of pure annihilation decays $\bar{B}_s^0 \to \pi\pi, \rho\pi$ and the well-measured decays $\bar{B}_s^0 \to \pi^- K^+, K^- K^+$ are given in the third column of Table I. The theoretical uncertainties are mainly induced by the three parts: quark masses, CKM elements and decay constants, and form factors. We first scan randomly the points in the allowed ranged of the input parameters of the three parts, respectively, and then add errors in quadrature.

Our QCDF results of scenarios $\overline{S4}$ listed in Table I are consistent with the former predictions given in Refs. [12,17], and the small difference is mainly induced by the different input values and some corrections mentioned above. One may find most of the predictions agree well with the experimental measurements. However, we again find the theoretical prediction $\mathcal{B}(\bar{B}_s^0 \to \pi^+\pi^-) \sim 0.21 \times 10^{-6}$, which agrees well with the other theoretical results such as $\sim 0.26 \times 10^{-6}$ in Ref. [17] and $\sim 0.155 \times 10^{-6}$ in Ref. [12], and is about 3.7σ lower than the average of experimental data $(0.73 \pm 0.14) \times 10^{-6}$.

Figure 1 shows the dependence of the measured observables of $\bar{B}_s^0 \to PP$ decays on the phase ϕ_s^{PP} with different ρ_s^{PP} values. From Fig. 1(a), one may easily find that the annihilation correction with the nominal annihilation

TABLE I. The numerical results for the branching fractions $[\times 10^{-6}]$ and the direct CP violations $[\times 10^{-2}]$ of $\bar{B}_s^0 \to \pi\pi$, $\rho\pi$, $\rho\rho$, $\pi^- K^+$, and $K^- K^+$ decays in each scenario.

	Experiment	Scheme I			Scheme II
		$\overline{S4}$	$S^{PP}A$	$S^{PP}B$	$m_g = 0.48$ GeV
$\mathcal{B}(\bar{B}_s^0 \to \pi^+\pi^-)$	0.73 ± 0.14	$0.21^{+0.05}_{-0.04}$	$0.69^{+0.16}_{-0.16}$	$0.66^{+0.17}_{-0.15}$	$0.50^{+0.11}_{-0.10}$
$\mathcal{B}(\bar{B}_s^0 \to \pi^0\pi^0)$	...	$0.10^{+0.02}_{-0.02}$	$0.34^{+0.08}_{-0.08}$	$0.33^{+0.08}_{-0.07}$	$0.25^{+0.05}_{-0.05}$
$\mathcal{B}(\bar{B}_s^0 \to \pi^+\rho^-)$	...	$0.010^{+0.002}_{-0.002}$	$0.032^{+0.008}_{-0.007}$	$0.036^{+0.009}_{-0.008}$	$0.028^{+0.007}_{-0.006}$
$\mathcal{B}(\bar{B}_s^0 \to \pi^-\rho^+)$	...	$0.011^{+0.003}_{-0.002}$	$0.046^{+0.013}_{-0.011}$	$0.019^{+0.005}_{-0.004}$	$0.028^{+0.007}_{-0.006}$
$\mathcal{B}(\bar{B}_s^0 \to \pi^0\rho^0)$	...	$0.010^{+0.002}_{-0.002}$	$0.037^{+0.010}_{-0.008}$	$0.025^{+0.006}_{-0.006}$	$0.028^{+0.007}_{-0.006}$
$A_{CP}(\bar{B}_s^0 \to \pi^+\pi^-)$	...	0	0	0	0
$A_{CP}(\bar{B}_s^0 \to \pi^0\pi^0)$	...	0	0	0	0
$A_{CP}(\bar{B}_s^0 \to \pi^+\rho^-)$	...	-12^{+1}_{-1}	-30^{+3}_{-3}	-15^{+1}_{-1}	0
$A_{CP}(\bar{B}_s^0 \to \pi^-\rho^+)$	...	11^{+1}_{-1}	21^{+2}_{-2}	30^{+3}_{-3}	0
$A_{CP}(\bar{B}_s^0 \to \pi^0\rho^0)$	...	0	0	0	0
$\mathcal{B}(\bar{B}_s^0 \to \pi^- K^+)$	5.0 ± 1.1	$5.9^{+0.9}_{-0.7}$	$5.4^{+0.9}_{-0.7}$	$5.3^{+1.0}_{-0.8}$	$6.2^{+0.9}_{-0.7}$
$\mathcal{B}(\bar{B}_s^0 \to K^- K^+)$	25.4 ± 3.7	$21.9^{+3.9}_{-3.8}$	$23.8^{+6.1}_{-5.8}$	$27.1^{+7.5}_{-6.6}$	$27.8^{+5.2}_{-5.1}$
$A_{CP}(\bar{B}_s^0 \to \pi^- K^+)$	39 ± 17	19^{+3}_{-3}	56^{+7}_{-8}	42^{+33}_{-19}	32^{+4}_{-5}
$A_{CP}(\bar{B}_s^0 \to K^- K^+)$	...	-8^{+1}_{-1}	-22^{+2}_{-4}	-6^{+4}_{-33}	-11^{+2}_{-1}

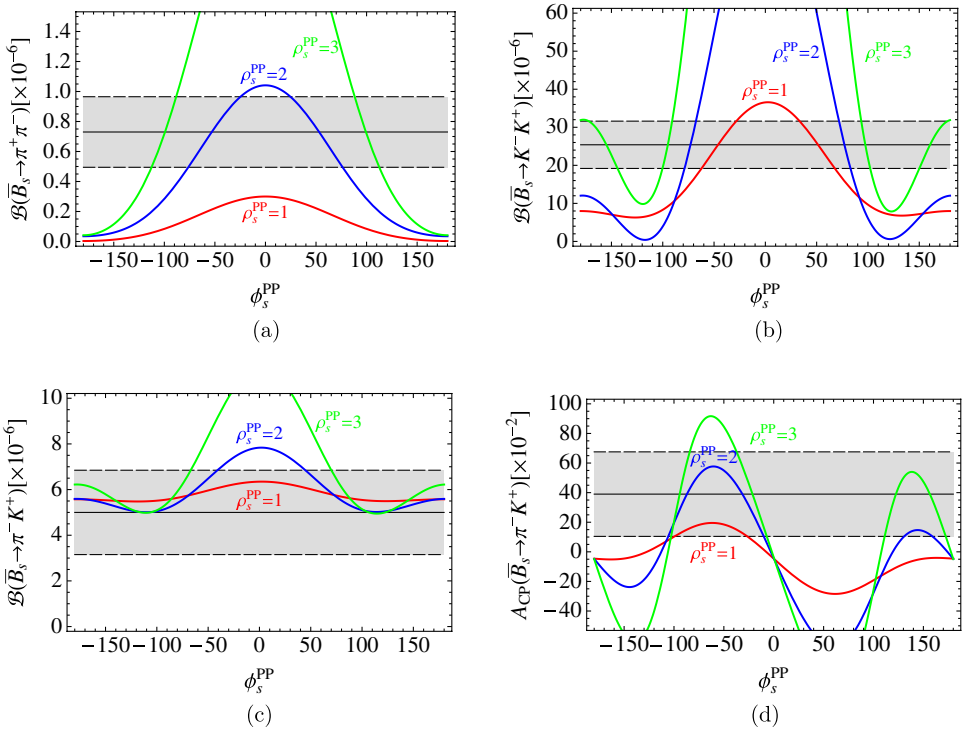

FIG. 1 (color online). The dependence of $\mathcal{B}(\bar{B}_s^0 \to \pi^+\pi^-, K^+K^-, \pi^-K^+)$ and $A_{CP}(\bar{B}_s^0 \to \pi^-K^+)$ on the phases ϕ_s^{PP} with different ρ_s^{PP} values. The dashed lines correspond to the error bars (1.68σ).

parameter value $\rho_s^{PP} \sim 1$ can hardly account for the measured large $\mathcal{B}(\bar{B}_s^0 \to \pi^+\pi^-)$ within errors, and a larger ρ_s^{PP} is required. For the other measured observables, as Figs. 1(b)–1(d) show, the large annihilation correction is not essential and is allowed. So, it is worthwhile to evaluate the exact values of the annihilation parameters with the constraints from the available experimental information of $\bar{B}_s^0 \to PP$ decays.

To keep the predictive power of the QCDF framework, we assume the annihilation parameters are universal for all of the $\bar{B}_s^0 \to PP$ decay channels in this paper. Under the constraints from $\mathcal{B}(\bar{B}_s^0 \to \pi^+\pi^-, \pi^-K^+, K^+K^-)$, $A_{CP}(\bar{B}_s^0 \to \pi^-K^+)$, and their combination, the allowed regions for the annihilation parameters ϕ_s^{PP} and ρ_s^{PP} are shown by Figs. 2(a) and 2(c) respectively. From Fig. 2(a), we find that the traditional treatment $\rho^{PP} \leqslant 1$ is allowed by the experimental results of $\mathcal{B}(\bar{B}_s^0 \to \pi^-K^+, K^+K^-)$ and $A_{CP}(\bar{B}_s^0 \to \pi^-K^+)$, but obviously excluded by recent experimental measurements $\mathcal{B}(\bar{B}_s^0 \to \pi^+\pi^-) = 0.73 \pm 0.14$. Combining the constraints from the four observables above, as Fig. 2(c) shows, the annihilation parameters are tightly restricted, and two solutions, named S$^{\rm PP}$A and B, respectively, are obtained as[1]

$$\begin{aligned} &\rho_s^{PP} = 2.5 \pm 0.8, \quad &&\phi_s^{PP} = -84^\circ \pm 21^\circ; \quad &&(S^{PP}A), \\ &\rho_s^{PP} = 3.5 \pm 0.3, \quad &&\phi_s^{PP} = 116^\circ \pm 9^\circ, \quad &&(S^{PP}B). \end{aligned} \tag{18}$$

Both of them imply a large annihilation correction is essential to accommodate the measured $\bar{B}_s \to PP$ decays.

As a comparison, we also evaluate the values of the annihilation parameters in $\bar{B}_d^0 \to PP$ decays with the constraints from the well-measured $\bar{B}_d^0 \to \pi^+K^-$ and recently measured $\bar{B}_d^0 \to K^+K^-$ decays. From Fig. 2(b), we find ϕ_d^{PP} and ρ_d^{PP} are bounded strongly by the precise experimental data of the branching fraction and direct CP asymmetry of the $\bar{B}_d^0 \to \pi^+K^-$ decay. Meanwhile, the constraint from $\mathcal{B}(\bar{B}_d^0 \to K^+K^-)$ is weak due to the rough measurement. Corresponding to the allowed region for ϕ_d^{PP} and ρ_d^{PP} shown by Fig. 2(c), we get the numerical results

$$\rho_d^{PP} = 1.2 \pm 0.3, \qquad \phi_d^{PP} = -48^\circ \pm 16^\circ, \tag{19}$$

which is similar to the result of scenario $\overline{S4}$ given by Eq. (12), while significantly different from those by B_s decays ϕ_s^{PP} and ρ_s^{PP} in Eq. (18).

For $\bar{B}_s^0 \to PV$ decay modes, so far, no available experimental measurement could be used to put a constraint on the annihilation parameters therein. Thus, in our numerical evaluations, we assume that the differences between $\rho(\phi)^{PV,VP}$ and $\rho(\phi)^{PP}$ in $\bar{B}_s^0$ decays are the same as the ones in $\bar{B}_d^0$ decays of scenario $\overline{S4}$ given by Eqs. (12) and (13), i.e.,

[1]Our fitting for the annihilation parameters is performed with the experimental data allowed within their respective 1.68σ ($\simeq 90\%$ C.L.) error bars, while the theoretical uncertainties are also considered by varying the input parameters within their respective regions specified in Appendix B.

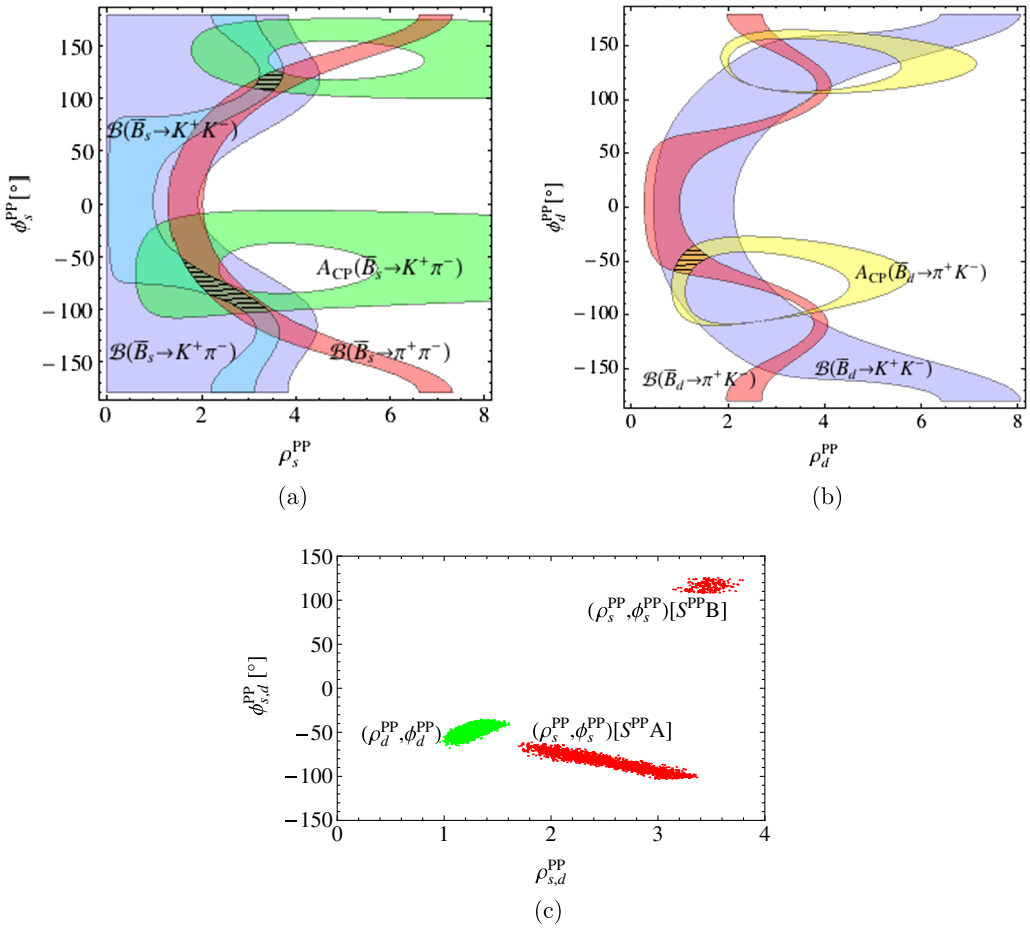

FIG. 2 (color online). The allowed regions for the annihilation parameters $\phi_{s,d}^{PP}$ and $\rho_{s,d}^{PP}$ under the constraints from the observables labeled in (a) and (b), respectively, and their combination (c).

$$\rho_s^{PV}=\rho_s^{VP}=\rho_s^{PP},\qquad \phi_s^{PV}=\phi_s^{PP}+35^\circ,\qquad \phi_s^{VP}=\phi_s^{PP}-15^\circ. \tag{20}$$

With the default values of $\rho_s^{PP,PV,VP}$ and $\phi_s^{PP,PV,VP}$ given by Eqs. (18) and (20) as inputs, we present our results of the observables in the fourth and fifth columns of Table I. We find that $\mathcal{B}(\bar{B}_s^0\to\pi^+\pi^-)$ could be enhanced to 0.7×10^{-6} to match the experimental data with large annihilation parameters within QCDF. Furthermore, all of the other theoretical results are in good agreement with the experimental data. The branching fractions of $\bar{B}_s^0\to PV$ decays, which may play an important role to confirm or refute the large annihilation corrections, are too small $\sim\mathcal{O}(10^{-8})$ to be measured very soon at LHCb.

B. Within scheme II

An alternative to the parametrization method, the endpoint divergency could be regulated by an infrared finite dynamical gluon propagator, which has been successfully applied to the B meson nonleptonic decays [13,14,20]. In this paper we adopt Cornwall's description for the gluon propagator, which is given by [21]

$$D(q^2)=\frac{1}{q^2-M_g^2(q^2)+i\epsilon}, \tag{21}$$

with the dynamical gluon mass

$$M_g^2(q^2)=m_g^2\left[\frac{\ln\left(\frac{q^2+4m_g^2}{\Lambda_{\rm QCD}^2}\right)}{\ln\left(\frac{4m_g^2}{\Lambda_{\rm QCD}^2}\right)}\right]^{-\frac{12}{11}}, \tag{22}$$

where q^2 is the gluon momentum square, which is spacelike in the hard spectator scattering contributions and timelike in the annihilation corrections. The corresponding strong coupling constant reads

$$\alpha_s(q^2)=\frac{4\pi}{\beta_0\ln\left(\frac{q^2+4M_g^2(q^2)}{\Lambda_{\rm QCD}^2}\right)}, \tag{23}$$

where $\beta_0=11-\frac{2}{3}n_f$ is the first coefficient of the beta function, and n_f the number of active flavors.

With the description given above, the amplitudes of the hard spectator scattering contributions and annihilation corrections in the $B\to PP$ and PV decays have been derived in Ref. [14]. Within this scheme, it is found that

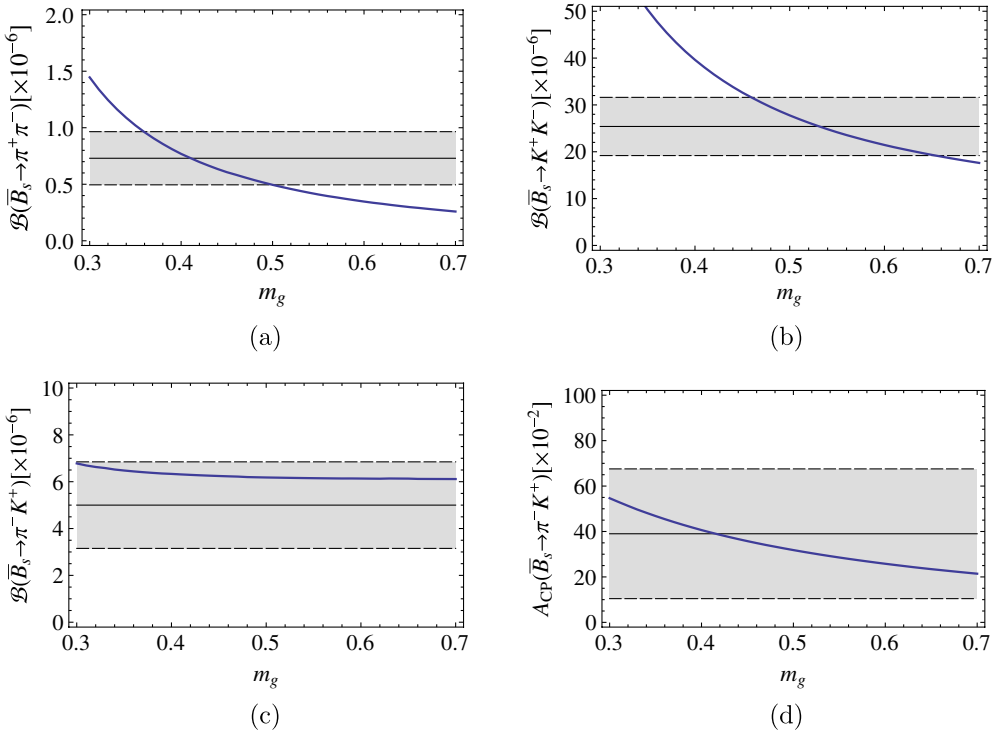

FIG. 3 (color online). The dependence of the measured observables of the $\bar{B}_s^0 \to PP$ decays on the effective gluon mass scale. The dashed lines correspond to the error bars (1.68σ).

the hard spectator scattering contributions are real and the annihilation corrections are complex with a large imaginary part [14]. Moreover, the strength of the annihilation correction is sensitive to the sole input parameter, the effective gluon mass scale m_g, whose typical value is 0.5 ± 0.2 GeV, obtained by relating the gluon mass to the gluon condensate [21]. Interestingly, in a B meson system, with the constraints from $B_{u,d} \to \pi K$, πK^*, and ρK decays, a reasonable similar result $m_g = 0.5 \pm 0.05$ GeV is found in Ref. [14]. So, as a cross-check, it is worthwhile to evaluate the value of the effective gluon mass scale m_g in $\bar{B}_s^0$ decays.

With $m_g = [0.3, 0.7]$ GeV allowed, the dependences of the measured observables $\mathcal{B}(\bar{B}_s^0 \to \pi^+\pi^-, K^+K^-, \pi^-K^+)$ and $A_{CP}(\bar{B}_s^0 \to \pi^- K^+)$ on m_g are shown in Fig. 3. From Fig. 3(a), we find that a small $m_g \sim 0.43$ GeV, which would lead to large annihilation corrections, is required by large experimental data $\mathcal{B}(\bar{B}_s^0 \to \pi^+\pi^-) = 0.73 \pm 0.14$. Meanwhile, as Fig. 3(b) shows, a relatively large $m_g \sim 0.52$ GeV could result in a good agreement between the theoretical prediction and experimental data for $\mathcal{B}(\bar{B}_s^0 \to K^+K^-)$. With the experimental errors considered, one also could find a common solution

$$m_g = 0.48 \pm 0.02 \text{ GeV}, \tag{24}$$

where its upper limit is dominated by $\mathcal{B}(\bar{B}_s^0 \to \pi^+\pi^-)$, and the lower one is dominated by $\mathcal{B}(\bar{B}_s^0 \to K^+K^-)$. Moreover, since a larger annihilation strength is required by $\mathcal{B}(\bar{B}_s^0 \to \pi^+\pi^-)$, such a solution is a bit smaller than the finding $m_g = 0.5 \pm 0.05$ GeV in $B_{u,d}$ decays [14], although they are also in agreement. Due to the dominance of the tree contribution α_1 in the amplitude of the $\bar{B}_s^0 \to \pi^+K^-$ decay, the effect of the annihilation contributions related to m_g to $\mathcal{B}(\bar{B}_s^0 \to \pi^+K^-)$ is negligible, which can be seen from Fig. 3(c). Furthermore, as Fig. 3(d) shows, because of the large experimental error, the constraint from $A_{CP}(\bar{B}_s^0 \to \pi^+K^-)$ on m_g is weak, too.

Taking $m_g = 0.48$ GeV, our numerical results for the observables are listed in the sixth column of Table I. One may find that all of the results are in good agreement with the experimental data, and most of them are similar to the scenarios $S^{PP}A$ and $S^{PP}B$ in scheme I. Within scheme I, $A_{CP}(\bar{B}_s^0 \to \pi^+\rho^-)$ and $A_{CP}(\bar{B}_s^0 \to \pi^-\rho^+)$ could be large due to the assumption that $\phi_s^{PV} \neq \phi_s^{VP}$, which can be seen from Eq. (20). However, within scheme II, we find that $A_{CP}(\bar{B}_s^0 \to \pi^+\rho^-) = A_{CP}(\bar{B}_s^0 \to \pi^-\rho^+) \approx 0$ with any value of m_g. The significantly different predictions for such two observables within two schemes will possibly be judged by the running LHCb and upcoming super-B experiments.

IV. $\bar{B}_s^0 \to VV$ DECAY MODES

Compared with $B \to PP$ and PV decays, the $B \to VV$ decays involve more observables, which are sensitive probes for testing the SM and various calculation approaches. Recently, $\bar{B}_s^0 \to K^{*0}\bar{K}^{*0}$ and $\phi\phi$ decays have been measured by LHCb and CDF collaborations, respectively [22]:

TABLE II. The numerical results for the branching fractions $\mathcal{B}[\times 10^{-6}]$, the direct CP violations $A_{CP}[\times 10^{-2}]$, and longitudinal and transverse polarization fractions $f_{L,\perp}[\times 10^{-2}]$ for $\bar{B}_s^0 \to \rho\rho$, $K^{*0}\bar{K}^{*0}$, and $\phi\phi$ decays in each scenarios.

	Experiment	Scheme I					Scheme II
		$\overline{S4}$	$S^{VV}A$	$S^{VV}B$	$S^{VV}C$	$S^{VV}D$	$m_g = 0.50$ GeV
$\mathcal{B}(\bar{B}_s^0 \to \rho^+\rho^-)$	$\cdots$	$0.36^{+0.12}_{-0.09}$	$0.24^{+0.12}_{-0.09}$	$0.66^{+0.22}_{-0.18}$	$0.67^{+0.23}_{-0.18}$	$0.21^{+0.10}_{-0.08}$	$1.30^{+0.44}_{-0.34}$
$\mathcal{B}(\bar{B}_s^0 \to \rho^0\rho^0)$	$\cdots$	$0.18^{+0.06}_{-0.05}$	$0.12^{+0.06}_{-0.04}$	$0.33^{+0.11}_{-0.09}$	$0.33^{+0.11}_{-0.09}$	$0.10^{+0.05}_{-0.04}$	$0.65^{+0.22}_{-0.17}$
$A_{CP}(\bar{B}_s^0 \to \rho^+\rho^-)$	$\cdots$	0	0	0	0	0	0
$A_{CP}(\bar{B}_s^0 \to \rho^0\rho^0)$	$\cdots$	0	0	0	0	0	0
$f_L(\bar{B}_s^0 \to \rho^+\rho^-)$	$\cdots$	99^{+0}_{-0}	96^{+0}_{-1}	98^{+0}_{-0}	98^{+0}_{-0}	97^{+1}_{-1}	98^{+0}_{-0}
$f_L(\bar{B}_s^0 \to \rho^0\rho^0)$	$\cdots$	99^{+0}_{-0}	96^{+0}_{-1}	98^{+0}_{-0}	98^{+0}_{-0}	97^{+1}_{-1}	98^{+0}_{-0}
$\mathcal{B}(\bar{B}_s^0 \to K^{*0}\bar{K}^{*0})$	28.1 ± 6.5	$11.0^{+2.9}_{-2.6}$	$16.7^{+6.5}_{-5.0}$	$15.3^{+4.9}_{-3.7}$	$15.9^{+5.4}_{-3.7}$	$15.9^{+6.5}_{-4.9}$	$20.6^{+6.5}_{-5.2}$
$\mathcal{B}(\bar{B}_s^0 \to \phi\phi)$	23.2 ± 8.4	$21.9^{+10.6}_{-4.6}$	$41.6^{+18.8}_{-12.0}$	$39.7^{+19.0}_{-10.0}$	$38.0^{+15.7}_{-10}$	$41.9^{+19.4}_{-12.0}$	$49.9^{+25.6}_{-13.3}$
$A_{CP}(\bar{B}_s^0 \to K^{*0}\bar{K}^{*0})$	$\cdots$	$0.8^{+0.1}_{-0.1}$	$-0.1^{+0.1}_{-0.0}$	$0.6^{+0.1}_{-0.1}$	$0.1^{+0.2}_{-0.1}$	$0.5^{+0.1}_{-0.1}$	$0.5^{+0.1}_{-0.1}$
$A_{CP}(\bar{B}_s^0 \to \phi\phi)$	$\cdots$	$0.9^{+0.2}_{-0.1}$	$-0.1^{+0.2}_{-0.0}$	$0.6^{+0.3}_{-0.1}$	$-0.0^{+0.2}_{-0.1}$	$0.5^{+0.3}_{-0.1}$	$0.5^{+0.2}_{-0.1}$
$f_L(\bar{B}_s^0 \to K^{*0}\bar{K}^{*0})$	31 ± 13	71^{+7}_{-7}	41^{+4}_{-3}	42^{+10}_{-6}	45^{+10}_{-7}	$38^{+3.3}_{-1.8}$	65^{+7}_{-6}
$f_L(\bar{B}_s^0 \to \phi\phi)$	34.8 ± 4.6	56^{+11}_{-8}	36^{+4}_{-3}	34^{+7}_{-3}	32^{+8}_{-2}	35^{+4}_{-3}	57^{+9}_{-4}
$f_\perp(\bar{B}_s^0 \to K^{*0}\bar{K}^{*0})$	38 ± 12	13^{+4}_{-4}	27^{+2}_{-2}	26^{+3}_{-5}	24^{+4}_{-4}	29^{+2}_{-2}	15^{+3}_{-3}
$f_\perp(\bar{B}_s^0 \to \phi\phi)$	36.5 ± 5.2	21^{+4}_{-5}	31^{+2}_{-2}	31^{+2}_{-4}	32^{+2}_{-4}	32^{+2}_{-2}	21^{+2}_{-4}

$$\begin{cases} \mathcal{B}(\bar{B}_s^0 \to K^{*0}\bar{K}^{*0}) = (28.1 \pm 4.6(\text{stat}) \pm 4.5(\text{syst}) \pm 3.4(f_s/f_d)) \times 10^{-6} \\ f_L(\bar{B}_s^0 \to K^{*0}\bar{K}^{*0}) = 0.31 \pm 0.12(\text{stat}) \pm 0.04(\text{syst}) \\ f_\perp(\bar{B}_s^0 \to K^{*0}\bar{K}^{*0}) = 0.38 \pm 0.11(\text{stat}) \pm 0.04(\text{syst}) \end{cases} \quad \text{LHCb;} \tag{25}$$

and [23]

$$\begin{cases} \mathcal{B}(\bar{B}_s^0 \to \phi\phi) = (23.2 \pm 1.8(\text{stat}) \pm 8.2(\text{syst})) \times 10^{-6} \\ f_L(\bar{B}_s^0 \to \phi\phi) = 0.348 \pm 0.041(\text{stat}) \pm 0.021(\text{syst}) \\ f_\perp(\bar{B}_s^0 \to \phi\phi) = 0.365 \pm 0.044(\text{stat}) \pm 0.027(\text{syst}) \end{cases} \quad \text{CDF.} \tag{26}$$

Because of the left-handedness of the weak interaction and the fact that the high-energy QCD interactions conserve helicity, the SM expects the dominance of the longitudinal amplitude and the transverse amplitudes are suppressed by the factor $m_{\phi,\bar{K}^{*0}}/m_B$, which significantly conflicts with the LHCb and CDF observation $f_L(\bar{B}_s^0 \to K^{*0}\bar{K}^{*0}, \phi\phi) \sim f_\perp(\bar{B}_s^0 \to K^{*0}\bar{K}^{*0}, \phi\phi)$. Therefore, it is worthy to perform a detailed evaluation within QCDF, and check if the tension could be moderated by annihilation corrections.

A. Within scheme I

With the annihilation parameters given by Eq. (17), the prediction of scenarios $\overline{S4}$ for $\bar{B}_s^0 \to \rho\rho$, $K^{*0}\bar{K}^{*0}$, and $\phi\phi$ decays are listed in the third column of Table II and agree with the former results of the QCDF [15,17]. One may find that there are no significant direct CP asymmetries for these decay modes, and the longitudinal polarization fractions of $\bar{B}_s^0 \to \rho\rho$ decays are close to unity. The branching fraction of the $\bar{B}_s^0 \to \phi\phi$ decay agrees well with the experimental data. Meanwhile, the default result $\mathcal{B}(\bar{B}_s^0 \to K^{*0}\bar{K}^{*0}) \sim 11.0 \times 10^{-6}$ is significantly smaller than the LHCb measurement $\sim 28.1 \times 10^{-6}$. However, one may notice that the uncertainties in the experimental measurement are still very large. For their polarization fractions, as expected above, the prediction of scenarios $\overline{S4}$ implies $f_L(\bar{B}_s^0 \to K^{*0}\bar{K}^{*0}, \phi\phi) \sim 0.71, 0.56 > f_\perp(\bar{B}_s^0 \to K^{*0}\bar{K}^{*0}, \phi\phi) \sim 0.13, 0.21$, which conflict with the LHCb and CDF observation $f_L(\bar{B}_s^0 \to K^{*0}\bar{K}^{*0}, \phi\phi) \approx f_\perp(\bar{B}_s^0 \to K^{*0}\bar{K}^{*0}, \phi\phi)$. In the following, we perform a detailed evaluation to check whether such a discrepancy could be moderated by the annihilation corrections.

The dependence of $\mathcal{B}(\bar{B}_s^0 \to K^{*0}\bar{K}^{*0}, \phi\phi)$ and $f_L(\bar{B}_s^0 \to K^{*0}\bar{K}^{*0}, \phi\phi)$ on the annihilation parameters is shown by Fig. 4. Comparing Fig. 4(b) with 4(d), we find the constraint from $f_L(\bar{B}_s^0 \to K^{*0}\bar{K}^{*0})$ on the annihilation parameters is weak due to its large experimental uncertainties. From Fig. 4(d), one may find the phase $\phi_s^{VV} \sim -40°$ or $50°$ with any value of ρ_s^{VV} could be helpful to moderate the tension between the theoretical prediction and experimental result for $f_L(\bar{B}_s^0 \to \phi\phi)$. With such a ϕ_s^{VV} value, as

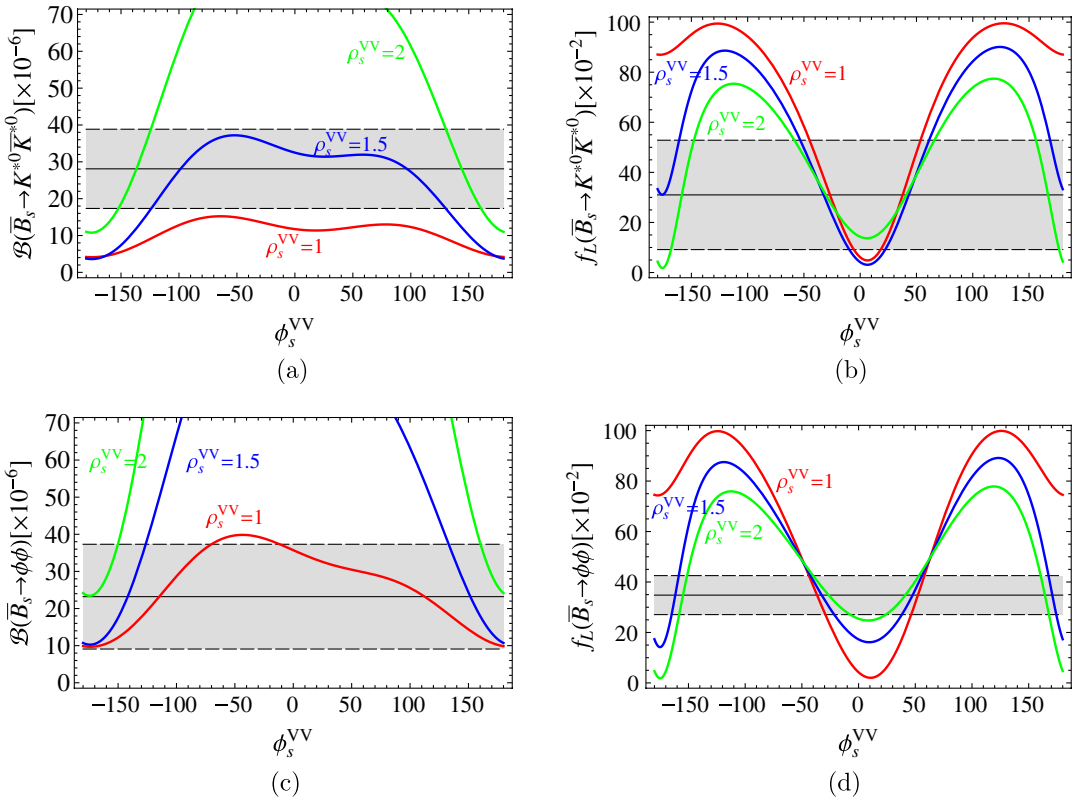

FIG. 4 (color online). The dependence of $\mathcal{B}(\bar{B}_s^0 \to K^{*0}\bar{K}^{*0}, \phi\phi)$ and $f_L(\bar{B}_s^0 \to K^{*0}\bar{K}^{*0}, \phi\phi)$ on the phases ϕ_s^{VV} with different ρ_s^{VV} values. The dashed lines correspond to the error bars (1.68σ).

shown in Figs. 4(a) and 4(c), a small $\rho_s^{VV} \sim 1$ is required by both $\mathcal{B}(\bar{B}_s^0 \to K^{*0}\bar{K}^{*0})$ and $\mathcal{B}(\bar{B}_s^0 \to \phi\phi)$. Furthermore, compared with such solutions, we find a larger $\rho_s^{VV} \sim 2$ with a larger phase $\phi_s^{VV} \sim -150°$ or $160°$ are also possible solutions. A detailed numerical examination is performed in the following.

Under the constraints from $\mathcal{B}(\bar{B}_s^0 \to K^{*0}\bar{K}^{*0}, \phi\phi)$ and $f_L(\bar{B}_s^0 \to K^{*0}\bar{K}^{*0}, \phi\phi)$, the allowed regions for the annihilation parameters are shown in Fig. 5. As shown in Fig. 5(a), the space of the annihilation parameters are strictly restricted. The upper and the lower limits of ρ_s^{VV} are dominated by $\mathcal{B}(\bar{B}_s^0 \to \phi\phi)$ and $\mathcal{B}(\bar{B}_s^0 \to K^{*0}\bar{K}^{*0})$, respectively. Meanwhile, the ranges of ϕ_s^{VV} are dominated by $f_L(\bar{B}_s^0 \to \phi\phi)$. Finally, under their combined constraints, we could find four solutions shown by Fig. 5(b). The corresponding numerical results are

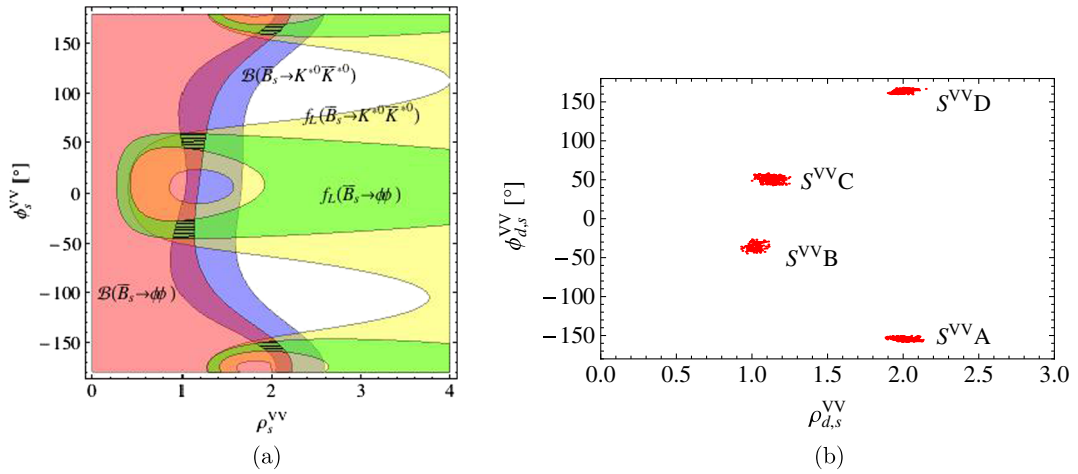

FIG. 5 (color online). The allowed regions for the annihilation parameters ϕ_s^{VV} and ρ_s^{VV} under the constraints from (a) $\mathcal{B}(\bar{B}_s^0 \to K^{*0}\bar{K}^{*0}, \phi\phi)$, $f_L(\bar{B}_s^0 \to K^{*0}\bar{K}^{*0}, \phi\phi)$, and (b) their combination, respectively.

$$\rho_s^{VV} = 2.0 \pm 0.1, \quad \phi_s^{VV} = -154^\circ \pm 4^\circ \quad (\mathrm{S^{VV}A}),$$
$$\rho_s^{VV} = 1.0 \pm 0.1, \quad \phi_s^{VV} = -36^\circ \pm 9^\circ \quad (\mathrm{S^{VV}B}),$$
$$\rho_s^{VV} = 1.1 \pm 0.1, \quad \phi_s^{VV} = 50^\circ \pm 7^\circ \quad (\mathrm{S^{VV}C}),$$
$$\rho_s^{VV} = 2.0 \pm 0.1, \quad \phi_s^{VV} = 164^\circ \pm 4^\circ \quad (\mathrm{S^{VV}D}). \tag{27}$$

With the default values of the annihilation parameters given by Eq. (27), our predictions of scheme I are summarized in Table II. We find that $f_L(\bar{B}_s^0 \to K^{*0}\bar{K}^{*0}, \phi\phi)$ could reduce to the experimental data by the annihilation contributions. Meanwhile, $f_\perp(\bar{B}_s^0 \to K^{*0}\bar{K}^{*0}, \phi\phi)$ are also significantly enhanced, and agree well with the experimental data. However, similar to the case in scenarios $\overline{S4}$, the result of $\mathcal{B}(\bar{B}_s^0 \to \phi\phi)$ is larger than the one of $\mathcal{B}(\bar{B}_s^0 \to K^{*0}\bar{K}^{*0})$ by a factor of about 2. In the previous works, the theoretical predictions within both QCDF and pQCD frameworks, for example, [5,15,17]

$$\begin{cases} \mathcal{B}(\bar{B}_s^0 \to \phi\phi) = (21.8^{+1.1+30.4}_{-1.1-17.0}) \times 10^{-6} \\ \mathcal{B}(\bar{B}_s^0 \to K^{*0}\bar{K}^{*0}) = (9.1^{+0.5+11.3}_{-0.4-6.8}) \times 10^{-6} \end{cases} \quad \text{QCDF;} \tag{28}$$

$$\begin{cases} \mathcal{B}(\bar{B}_s^0 \to \phi\phi) = (16.7^{+2.6+11.3}_{-2.1-8.8}) \times 10^{-6} \\ \mathcal{B}(\bar{B}_s^0 \to K^{*0}\bar{K}^{*0}) = (6.6^{+1.1+1.9}_{-1.4-1.7}) \times 10^{-6} \end{cases} \quad \text{QCDF;} \tag{29}$$

$$\begin{cases} \mathcal{B}(\bar{B}_s^0 \to \phi\phi) = (35.3^{+8.3+16.7+0.0}_{-6.9-10.2-0.0}) \times 10^{-6} \\ \mathcal{B}(\bar{B}_s^0 \to K^{*0}\bar{K}^{*0}) = (7.8^{+1.9+3.8+0.0}_{-1.5-2.2-0.0}) \times 10^{-6} \end{cases} \quad \text{pQCD,} \tag{30}$$

present a similar result that $\mathcal{B}(\bar{B}_s^0 \to \phi\phi) > \mathcal{B}(\bar{B}_s^0 \to K^{*0}\bar{K}^{*0})$, which is obviously inconsistent with the LHCb and CDF measurements Eqs. (25) and (26) that $\mathcal{B}(\bar{B}_s^0 \to \phi\phi) \simeq \mathcal{B}(\bar{B}_s^0 \to K^{*0}\bar{K}^{*0})$. Such a theoretical situation could be easily understood from their amplitudes given by Eqs. (A5) and (A6) in Appendix A. The amplitudes of both $\bar{B}_s^0 \to K^{*0}\bar{K}^{*0}$ and $\bar{B}_s^0 \to \phi\phi$ decays are dominated by the effective coefficients α_4^p, and annihilation contributions to them are similar. However, an additional overall factor 2 is included in the amplitude of $\bar{B}_s^0 \to \phi\phi$. So, $\mathcal{B}(\bar{B}_s^0 \to \phi\phi)$ would always be larger than $\mathcal{B}(\bar{B}_s^0 \to K^{*0}\bar{K}^{*0})$.

For the $\bar{B}_s^0 \to \rho\rho$ decays, their longitudinal polarization fractions are always close to unity within the four solutions. Meanwhile, the predictions of $\mathrm{S^{VV}B}$ and $\mathrm{S^{VV}C}$ for $\mathcal{B}(\bar{B}_s^0 \to \rho\rho)$ are significantly larger than the ones of $\mathrm{S^{VV}A}$ and $\mathrm{S^{VV}D}$. So, the four solutions for the annihilation parameters given by Eq. (27) could be tested by the upcoming LHCb measurements of $\mathcal{B}(\bar{B}_s^0 \to \rho\rho)$.

B. Within scheme II

With the infrared finite gluon propagator to deal with the endpoint divergences, the hard spectator and the annihilation corrections for $B \to PP$ and PV decays have been evaluated in Ref. [14]. Meanwhile, the ones for $B \to VV$ decays have not been calculated until now. So, firstly, we would recalculate these corrections within scheme II. With the same convention and notation as Refs. [14,15], the hard spectator scattering contributions can be expressed as

$$H_i^- = -\frac{2f_B f_{V_1}^\perp}{m_B m_b F_-^{B\to V_1}(0)} \int_0^1 dxdyd\xi \alpha_s(q^2) \times \frac{\Phi_{B1}\phi_1^\perp(x)\phi_{b2}(y)}{(\xi\bar{x} + \omega^2(q^2))\bar{x}y}, \tag{31}$$

for $i = 1, 2, 3, 4, 9, 10$;

$$H_i^- = \frac{2f_B f_{V_1}^\perp}{m_B m_b F_-^{B\to V_1}(0)} \int_0^1 dxdyd\xi \alpha_s(q^2) \times \frac{\Phi_{B1}\phi_1^\perp(x)\phi_{a2}(y)}{(\xi\bar{x} + \omega^2(q^2))\bar{x}\,\bar{y}}, \tag{32}$$

for $i = 5, 7$;

$$H_i^- = -\frac{f_B f_{V_1}}{m_B F_-^{B\to V_1}(0)} \frac{m_1}{m_2^2} \int_0^1 dxdyd\xi \alpha_s(q^2) \times \frac{\Phi_{B1}\phi_{a1}(x)\phi_2^\perp(y)}{(\xi\bar{x} + \omega^2(q^2))\bar{y}y}, \tag{33}$$

for $i = 6, 8$. In the equations above, $\omega^2(q^2) = M_g^2(q^2)/M_B^2$, $q^2 = -Q^2$, and $Q^2 \simeq -\xi\bar{x}M_B^2$ is the spacelike gluon momentum square in the scattering kernels. The function $\Phi_{B1}(\xi)$ is the B meson light-cone distribution amplitude, where ξ is the light-cone momentum fraction of the light antiquark in the B meson. In our following numerical evaluation, $\Phi_B(\xi) = N_B\xi(1-\xi)\exp[-(\frac{M_B}{M_B - m_b})^2(\xi - \xi_B)^2]$ [24] is used.

The longitudinal part of the annihilation amplitudes are given by

$$A_1^{i,0} = \pi \int_0^1 dxdy\alpha_s(q^2)\Big\{\Phi_{V1}(x)\Phi_{V2}(y) \times \Big[\frac{\bar{y}}{(x\bar{y} - \omega^2(q^2) + i\varepsilon)(1 - \bar{x}y)} + \frac{1}{\bar{y}(x\bar{y} - \omega^2(q^2) + i\varepsilon)}\Big] - r_\chi^{V_1} r_\chi^{V_2} \Phi_{v1}(x)\Phi_{v2}(y) \frac{2}{x\bar{y} - \omega^2(q^2) + i\varepsilon}\Big\}, \tag{34}$$

$$A_2^{i,0} = \pi \int_0^1 dxdy\alpha_s(q^2)\Big\{\Phi_{V1}(x)\Phi_{V2}(y) \times \Big[\frac{x}{(x\bar{y} - \omega^2(q^2) + i\varepsilon)(1 - \bar{x}y)} + \frac{1}{x(x\bar{y} - \omega^2(q^2) + i\varepsilon)}\Big] - r_\chi^{V_1} r_\chi^{V_2} \Phi_{v1}(x)\Phi_{v2}(y) \frac{2}{x\bar{y} - \omega^2(q^2) + i\varepsilon}\Big\}, \tag{35}$$

$$A_3^{i,0} = \pi \int_0^1 dxdy\alpha_s(q^2)\Big\{r_\chi^{V_1}\Phi_{v1}(x)\Phi_{V2}(y) \times \frac{2\bar{x}}{(x\bar{y}-\omega^2(q^2)+i\varepsilon)(1-\bar{x}y)} + r_\chi^{V_2}\Phi_{V1}(x)\Phi_{v2}(y) \times \frac{2y}{(x\bar{y}-\omega^2(q^2)+i\varepsilon)(1-\bar{x}y)}\Big\}, \quad (36)$$

$$A_3^{f,0} = \pi \int_0^1 dxdy\alpha_s(q^2)\Big\{r_\chi^{V_1}\Phi_{v1}(x)\Phi_{V2}(y) \times \frac{2(1+\bar{y})}{\bar{y}(x\bar{y}-\omega^2(q^2)+i\varepsilon)} - r_\chi^{V_2}\Phi_{V1}(x)\Phi_{v2}(y) \times \frac{2(1+x)}{x(x\bar{y}-\omega^2(q^2)+i\varepsilon)}\Big\}, \quad (37)$$

and $A_{1,2}^{f,0} = 0$. The nonvanishing transverse amplitudes are

$$A_1^{i,-} = \pi\frac{2m_1m_2}{m_B^2}\int_0^1 dxdy\alpha_s(q^2)\Big\{\phi_{b1}(x)\phi_{b2}(y) \times \Big[\frac{1+\bar{y}}{(1-\bar{x}y)(x\bar{y}-\omega^2(q^2)+i\varepsilon)} + \frac{\bar{x}\bar{y}^2}{(1-\bar{x}y)(x\bar{y}-\omega^2(q^2)+i\varepsilon)^2} - \frac{\bar{x}\bar{y}^2}{(1-\bar{x}y)^2(x\bar{y}-\omega^2(q^2)+i\varepsilon)} + \frac{\bar{x}}{(x\bar{y}-\omega^2(q^2)+i\varepsilon)^2}\Big]\Big\}, \quad (38)$$

$$A_2^{i,-} = \pi\frac{2m_1m_2}{m_B^2}\int_0^1 dxdy\alpha_s(q^2)\Big\{\phi_{a1}(x)\phi_{a2}(y) \times \Big[\frac{1+x}{(1-\bar{x}y)(x\bar{y}-\omega^2(q^2)+i\varepsilon)} + \frac{x^2y}{(1-\bar{x}y)(x\bar{y}-\omega^2(q^2)+i\varepsilon)^2} - \frac{x^2y}{(1-\bar{x}y)^2(x\bar{y}-\omega^2(q^2)+i\varepsilon)} + \frac{y}{(x\bar{y}-\omega^2(q^2)+i\varepsilon)^2}\Big]\Big\}, \quad (39)$$

$$A_3^{i,-} = \pi\int_0^1 dxdy\alpha_s(q^2)\Big\{\frac{2m_1}{m_2}r_\chi^{V_2}\phi_{a1}(x)\phi_2^\perp(y) \times \frac{1}{(x\bar{y}-\omega^2(q^2)+i\varepsilon)(1-\bar{x}y)} - \frac{2m_2}{m_1}r_\chi^{V_1}\phi_1^\perp(x)\phi_{b2}(y) \times \frac{1}{(x\bar{y}-\omega^2(q^2)+i\varepsilon)(1-\bar{x}y)}\Big\}, \quad (40)$$

$$A_3^{f,-} = \pi\int_0^1 dxdy\alpha_s(q^2)\Big\{\frac{2m_1}{m_2}r_\chi^{V_2}\phi_{a1}(x)\phi_2^\perp(y) \times \frac{1}{\bar{y}(x\bar{y}-\omega^2(q^2)+i\varepsilon)} + \frac{2m_2}{m_1}r_\chi^{V_1}\phi_1^\perp(x)\phi_{b2}(y) \times \frac{1}{x(x\bar{y}-\omega^2(q^2)+i\varepsilon)}\Big\}, \quad (41)$$

$$A_1^{i,+} = \pi\frac{2m_1m_2}{m_B^2}\int_0^1 dxdy\alpha_s(q^2)\Big\{\phi_{a1}(x)\phi_{a2}(y)\Big[\frac{\bar{y}}{(1-\bar{x}y)(x\bar{y}-\omega^2(q^2)+i\varepsilon)} + \frac{xy\bar{y}}{(1-\bar{x}y)(x\bar{y}-\omega^2(q^2)+i\varepsilon)^2} - \frac{xy\bar{y}}{(1-\bar{x}y)^2(x\bar{y}-\omega^2(q^2)+i\varepsilon)} + \frac{1}{\bar{y}^2(x\bar{y}-\omega^2(q^2)+i\varepsilon)} + \frac{xy}{\bar{y}(x\bar{y}-\omega^2(q^2)+i\varepsilon)^2}\Big]\Big\}, \quad (42)$$

$$A_2^{i,+} = \pi\frac{2m_1m_2}{m_B^2}\int_0^1 dxdy\alpha_s(q^2)\Big\{\phi_{b1}(x)\phi_{b2}(y)\Big[\frac{x}{(1-\bar{x}y)(x\bar{y}-\omega^2(q^2)+i\varepsilon)} + \frac{x\bar{x}\,\bar{y}}{(1-\bar{x}y)(x\bar{y}-\omega^2(q^2)+i\varepsilon)^2} - \frac{x\bar{x}\,\bar{y}}{(1-\bar{x}y)^2(x\bar{y}-\omega^2(q^2)+i\varepsilon)} + \frac{1}{x^2(x\bar{y}-\omega^2(q^2)+i\varepsilon)} + \frac{\bar{x}\,\bar{y}}{x(x\bar{y}-\omega^2(q^2)+i\varepsilon)^2}\Big]\Big\}, \quad (43)$$

where $q^2 \simeq x\bar{y}M_B^2$ is the timelike gluon momentum square. As found in Ref. [14], the hard spectator scattering contributions are real, but the annihilation contributions are complex with a large imaginary part. Their contributions are dominated by the value of the effective dynamical gluon mass scale m_g.

With the default values of the input parameters, the dependence of $\mathcal{B}(\bar{B}_s^0 \to K^{*0}\bar{K}^{*0}, \phi\phi)$ and $f_{L,\perp}(\bar{B}_s^0 \to K^{*0}\bar{K}^{*0}, \phi\phi)$ on the parameter m_g is shown by Fig. 6. From Figs. 6(b) and 6(c) we find that the QCDF predictions for $f_{L(\perp)}(\bar{B}_s^0 \to K^{*0}\bar{K}^{*0}, \phi\phi)$ could be reduced (enhanced) to the experimental measurements with a small effective dynamical gluon mass $m_g \lesssim 0.4$ GeV, which leads to a large annihilation contribution. Meanwhile, as Fig. 6(a) shows, a small m_g is also allowed by the constraint from $\mathcal{B}(\bar{B}_s^0 \to K^{*0}\bar{K}^{*0})$. However, such a small m_g value would induce too large $\mathcal{B}(\bar{B}_s^0 \to \phi\phi)$, which is much larger than the experimental data.

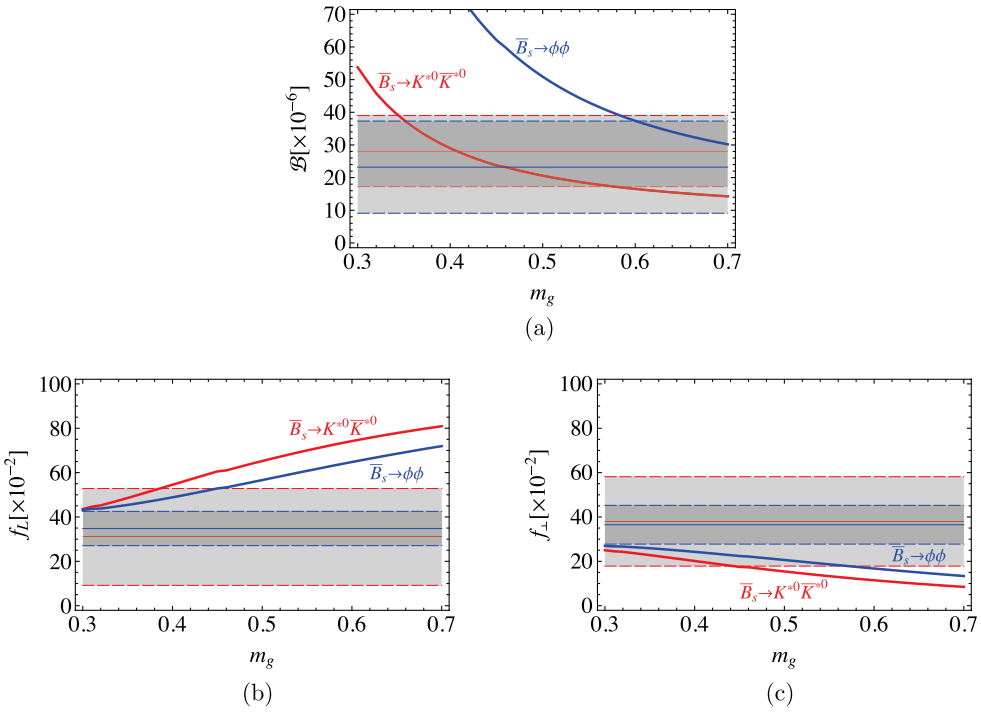

FIG. 6 (color online). The dependence of $\mathcal{B}(\bar{B}_s^0 \to K^{*0}\bar{K}^{*0}, \phi\phi)$ and $f_{L,\perp}(\bar{B}_s^0 \to K^{*0}\bar{K}^{*0}, \phi\phi)$ on the effective dynamical gluon mass scale. The dashed lines correspond to the error bars (1.68σ).

With a default m_g value 0.5 GeV, we present our predictions for the observables in the last column of Table II. We find that our prediction $\mathcal{B}(\bar{B}_s^0 \to K^{*0}\bar{K}^{*0}) = (20.6^{+6.5}_{-5.2}) \times 10^{-6}$ agrees well with the experimental data $(28.1 \pm 6.5) \times 10^{-6}$. However, unfortunately, $\mathcal{B}(\bar{B}_s^0 \to \phi\phi)$ is enhanced much by the annihilation corrections, whose lower limit $(49.9 - 13.3) \times 10^{-6}$ is about 1.6σ larger than the CDF measurement $(23.2 \pm 8.4) \times 10^{-6}$. In fact, with any m_g value, as analyzed in the last section, the theoretical prediction of $\mathcal{B}(\bar{B}_s^0 \to \phi\phi)$ is always much larger than $\mathcal{B}(\bar{B}_s^0 \to K^{*0}\bar{K}^{*0})$, which also can be seen from Fig. 6(a). Because a small m_g, which helps to accommodate the discrepancy of $f_{L,\perp}(\bar{B}_s^0 \to K^{*0}\bar{K}^{*0}, \phi\phi)$ between the theoretical predictions and experimental data as Figs. 6(b) and 6(c) show, is excluded by the constraint from $\mathcal{B}(\bar{B}_s^0 \to \phi\phi)$, the predictions of scheme II for $f_{L(\perp)}(\bar{B}_s^0 \to K^{*0}\bar{K}^{*0}, \phi\phi)$ are larger (smaller) than the experimental measurements, which is similar to the results of scenarios $\overline{S4}$. For the $\bar{B}_s^0 \to \rho\rho$ decays, their branching fractions in scheme II are significantly larger than the ones in scheme I. So, the upcoming measurements on $\mathcal{B}(\bar{B}_s^0 \to \rho\rho)$ could provide a judgment regarding the two schemes.

V. CONCLUSION

Motivated by the most recently observed large branching fraction of the pure annihilation decay $\bar{B}_s^0 \to \pi^+\pi^-$ and large transverse polarization fractions in the $\bar{B}_s^0 \to K^{*0}\bar{K}^{*0}$, $\phi\phi$ decays, we have revisited the hard spectator and annihilation corrections in nonleptonic $\bar{B}_s^0$ decays within a QCD factorization approach. In this paper, two schemes (parametrization and using an infrared finite gluon propagator) to model the effects of the end-point singularity in hard spectator and annihilation corrections have been evaluated. In our numerical evaluations, all of the pure annihilation and well-measured $\bar{B}_s^0$ decays have been studied in detail simultaneously. Our main conclusions are summarized as follows:

(i) For $\bar{B}_s^0 \to PP$ decays, within scheme I, due to the large $\mathcal{B}(\bar{B}_s^0 \to \pi^+\pi^-)$ measured by CDF and LHCb collaborations, a large annihilation parameter ρ_s^{PP} is required. Under the constraints from $\mathcal{B}(\bar{B}_s^0 \to \pi^+\pi^-, \pi^-K^+, K^-K^+)$ and $A_{CP}(\bar{B}_s^0 \to \pi^-K^+)$, two solutions $\rho_s^{PP} \sim 2.5(3.5)$ and $\phi_s^{PP} \sim -84°(116°)$ are found, which are significantly larger than the values $\rho^{PP} \sim 1$ and $\phi^{PP} \sim -55°$ adapted in the literature. With the obtained two solutions of the annihilation parameters given in Eq. (18), all of the QCDF predictions for $\bar{B}_s^0 \to PP$ decays agree well with the available experimental data.

(ii) For $\bar{B}_s^0 \to VV$ decays, within scheme I, the measured small $f_L(\bar{B}_s^0 \to K^{*0}\bar{K}^{*0}, \phi\phi)$ and large $f_\perp(\bar{B}_s^0 \to K^{*0}\bar{K}^{*0}, \phi\phi)$ could be accommodated by the annihilation contributions. With the constraints from $\mathcal{B}(\bar{B}_s^0 \to K^{*0}\bar{K}^{*0}, \phi\phi)$ and $f_{L,\perp}(\bar{B}_s^0 \to K^{*0}\bar{K}^{*0}, \phi\phi)$, we find four solutions of the annihilation parameters ρ_s^{VV} and ϕ_s^{VV} given by Eq. (27).

Some of these solutions will be confirmed or refuted by the upcoming LHCb measurement on $\bar{B}_s^0 \to \rho\rho$ decays.

(iii) Within scheme II, using the effective gluon mass $m_g = 0.48$ GeV, QCDF predictions for $\bar{B}_s^0 \to PP$ decays are found to be in good agreement with the available experimental results. Furthermore, some of its predictions are different from the ones in scheme I, such as the branching fractions and direct CP asymmetries of $\bar{B}_s^0 \to \rho\pi$ decays, which will be judged by the upcoming LHCb and proposed super-B experiments. For the $\bar{B}_s^0 \to VV$ decays, $f_{L,\perp}(\bar{B}_s^0 \to K^{*0}\bar{K}^{*0}, \phi\phi)$ could be accommodated by the annihilation contributions with a small $m_g \lesssim 0.4$ GeV, which unfortunately is excluded by $\mathcal{B}(\bar{B}_s^0 \to \phi\phi)$.

(iv) Within both schemes I and II, $\mathcal{B}(\bar{B}_s^0 \to \phi\phi)$ is always larger than $\mathcal{B}(\bar{B}_s^0 \to K^{*0}\bar{K}^{*0})$, which significantly conflicts with the LHCb and CDF observation $\mathcal{B}(\bar{B}_s^0 \to \phi\phi) \simeq \mathcal{B}(\bar{B}_s^0 \to K^{*0}\bar{K}^{*0})$. A similar situation is also presented in the pQCD approach, as summarized in Refs. [17,28–30]. Thus, the present experimental result $\mathcal{B}(\bar{B}_s^0 \to \phi\phi) \simeq \mathcal{B}(\bar{B}_s^0 \to K^{*0}\bar{K}^{*0})$ raises a challenge to theoretical approaches for B nonleptonic decay. Further refined measurements and theoretical studies are required to resolve such a possible anomaly.

.

ACKNOWLEDGMENTS

We are grateful to Hai-Yang Cheng and De-Shan Yang for helpful discussions. The work is supported by the National Natural Science Foundation under Grants No. 11075059 and 11105043, Research Fund for the Doctoral Program of Higher Education of China under Grant No. 20114104120002, and China Postdoctoral Science Foundation under Grant No. 2011M500118.

APPENDIX A: DECAY AMPLITUDES WITH QCDF

For the self-consistency of this paper, the following decay amplitudes are recapitulated from Refs. [12,15]. The amplitudes of $\bar{B}_s \to \pi\rho$ decays are

$$\mathcal{A}_{\bar{B}_s\to\pi^+\rho^-} = B_{\pi\rho}\left[b_4^p - \frac{1}{2}b_{4,\mathrm{EW}}^p\right] + B_{\rho\pi}[\delta_{pu}b_1 + b_4^p + b_{4,\mathrm{EW}}^p], \quad \text{(A1)}$$

$$2\mathcal{A}_{\bar{B}_s\to\pi^0\rho^0} = B_{\pi\rho}\left[\delta_{pu}b_1 + 2b_4^p + \frac{1}{2}b_{4,\mathrm{EW}}^p\right] + B_{\rho\pi}\left[\delta_{pu}b_1 + 2b_4^p + \frac{1}{2}b_{4,\mathrm{EW}}^p\right]. \quad \text{(A2)}$$

The amplitude of the $\bar{B}_s \to \pi^-\rho^+$ decay is obtained from the first expression by interchanging $(\pi) \leftrightarrow (\rho)$ everywhere. The expressions for the $\bar{B}_s \to \pi\pi$ and $\rho\rho$ amplitudes are obtained by setting $(\rho) \to (\pi)$ and $(\pi) \to (\rho)$, respectively.

The decay amplitudes of $\bar{B}_s \to \pi^-K^+$, K^-K^+, and $\bar{K}^{*0}K^{*0}$, $\phi\phi$ decays are

$$\mathcal{A}_{\bar{B}_s\to\pi^-K^+} = A_{K\pi}\left[\delta_{pu}\alpha_1 + \alpha_4^p + \alpha_{4,\mathrm{EW}}^p + \beta_3^p - \frac{1}{2}\beta_{3,\mathrm{EW}}^p\right], \quad \text{(A3)}$$

$$\mathcal{A}_{\bar{B}_s\to K^-K^+} = B_{K^-K^+}[\delta_{pu}b_1 + b_4^p + b_{4,\mathrm{EW}}^p] + A_{K^+K^-}\left[\delta_{pu}\alpha_1 + \alpha_4^p + \alpha_{4,\mathrm{EW}}^p + \beta_3^p + \beta_4^p + \frac{1}{2}\beta_{3,\mathrm{EW}}^p - \frac{1}{2}\beta_{4,\mathrm{EW}}^p\right], \quad \text{(A4)}$$

$$\mathcal{A}_{\bar{B}_s\to\bar{K}^{*0}K^{*0}} = B_{\bar{K}^{*0}K^{*0}}\left[b_4^p - \frac{1}{2}b_{4,\mathrm{EW}}^p\right] + A_{K^{*0}\bar{K}^{*0}}\left[\alpha_4^p - \frac{1}{2}\alpha_{4,\mathrm{EW}}^p + \beta_3^p + \beta_4^p - \frac{1}{2}\beta_{3,\mathrm{EW}}^p - \frac{1}{2}\beta_{4,\mathrm{EW}}^p\right], \quad \text{(A5)}$$

$$\mathcal{A}_{\bar{B}_s\to\phi\phi} = 2A_{\phi\phi}\left[\alpha_3^p + \alpha_4^p - \frac{1}{2}\alpha_{3,\mathrm{EW}}^p - \frac{1}{2}\alpha_{4,\mathrm{EW}}^p + \beta_3^p + \beta_4^p - \frac{1}{2}\beta_{3,\mathrm{EW}}^p - \frac{1}{2}\beta_{4,\mathrm{EW}}^p\right]. \quad \text{(A6)}$$

The explicit expressions for the coefficients $\alpha_i^p \equiv \alpha_i^p(M_1M_2)$ and $\beta_i^p \equiv \beta_i^p(M_1M_2)$ can be found in Refs. [12,15].

APPENDIX B: THEORETICAL INPUT PARAMETERS

For the CKM matrix elements, we adopt the CKMfitter Group's fitting results [25]:

$$\bar{\rho} = 0.144 \pm 0.025, \qquad \bar{\eta} = 0.342^{+0.016}_{-0.015},$$
$$A = 0.812^{+0.013}_{-0.027}, \qquad \lambda = 0.22543 \pm 0.00077. \quad \text{(B1)}$$

As for the quark mass, we take [28,26,27]

$$m_u = m_d = m_s = 0, \qquad m_c = 1.61^{+0.08}_{-0.12}\ \mathrm{GeV},$$
$$m_b = 4.78^{+0.21}_{-0.07}\ \mathrm{GeV}, \qquad m_t = 172.4 \pm 1.22\ \mathrm{GeV}, \quad \text{(B2)}$$

for the pole masses and

$$\frac{\bar{m}_s(\mu)}{\bar{m}_q(\mu)} = 27.4 \pm 0.4, \qquad \bar{m}_s(2\ \mathrm{GeV}) = 87 \pm 6\ \mathrm{MeV},$$
$$\bar{m}_c(\bar{m}_c) = 1.27^{+0.07}_{-0.09}\ \mathrm{GeV}, \qquad \bar{m}_b(\bar{m}_b) = 4.19^{+0.18}_{-0.06}\ \mathrm{GeV},$$
$$\bar{m}_t(\bar{m}_t) = 164.8 \pm 1.2\ \mathrm{GeV}, \quad \text{(B3)}$$

for the running masses, where $m_q = m_{u,d,s}$.

The decay constants are [29,30,26]

$$f_{B_s} = (231 \pm 15)\ \text{MeV}, \qquad f_{B_d} = (190 \pm 13)\ \text{MeV},$$
$$f_\pi = (130.4 \pm 0.2)\ \text{MeV}, \qquad f_K = (156.1 \pm 0.8)\ \text{MeV},$$
$$f_\rho = (209 \pm 2)\ \text{MeV}. \tag{B4}$$

As for the B-meson lifetimes, $\tau_{B_d} = 1.525$ ps and $\tau_{B_s} = 1.472$ ps are used. Furthermore, the form factor $F_0^{B\to\pi}(0) = 0.258 \pm 0.031$ [30] is used to evaluate the amplitude of $\bar{B}_d^0 \to \pi^+ K^-$ decay. For $\bar{B}_s^0 \to \pi^- K^+$, $K^- K^+$ decays, we shall use $F_0^{B_s\to K}(0) = 0.24$ obtained by both lattice and pQCD calculations and suggested by Ref. [17]. For the other decay constants and form factors related to $\bar{B}_s^0 \to K^{*0}\bar{K}^{*0}$ and $\bar{B}_s^0 \to \phi\phi$, we choose the similar inputs used in Ref. [15]. These values follow the QCD sum rule calculation Ref. [30], but some modifications within theoretical errors are made to improve the description of data. Their values are

$$f_{K^*} = (218 \pm 4)\ \text{MeV}, \qquad f_{K^*}^\perp(2\ \text{GeV}) = (175 \pm 25)\ \text{MeV}, \qquad f_\phi = (221 \pm 3)\ \text{MeV},$$
$$f_\phi^\perp(2\text{GeV}) = (175 \pm 25)\ \text{MeV}, \qquad A_0^{B_s\to\bar{K}^*} = 0.38 \pm 0.03, \qquad F_-^{B_s\to\bar{K}^*} = 0.53 \pm 0.05,$$
$$F_+^{B_s\to\bar{K}^*} = 0.00 \pm 0.06 \qquad A_0^{B_s\to\phi} = 0.38^{+0.10}_{-0.02}, \qquad F_-^{B_s\to\phi} = 0.65^{+0.14}_{-0.00}, \qquad F_+^{B_s\to\phi} = 0.00 \pm 0.06. \tag{B5}$$

[1] CDF Collaboration, Phys. Rev. Lett. **107**, 261802 (2011).
[2] LHCb Collaboration, Report No. LHCb-CONF-2011-042, 2011.
[3] E. Barberio *et al.* (HFAG), arXiv:1010.1589 (online update at http://www.slac.stanford.edu/xorg/hfag).
[4] G. H. Zhu, Phys. Lett. B **702**, 408 (2011).
[5] A. Ali, G. Kramer, Y. Li, C. D. Lu, Y. L. Shen, W. Wang, and Y. M. Wang, Phys. Rev. D **76**, 074018 (2007); Y. Li and C. D. Lu, Commun. Theor. Phys. **44**, 659 (2005).
[6] C. D. Lu, K. Ukai, and M. Z. Yang, Phys. Rev. D **63**, 074009 (2001).
[7] Z. J. Xiao, W. F. Wang, and Y. Y. Fan, Phys. Rev. D **85**, 094003 (2012).
[8] Y. Y. Keum, H. N. Li, and A. I. Sanda, Phys. Lett. B **504**, 6 (2001); Phys. Rev. D **63**, 054008 (2001).
[9] C. W. Bauer, S. Fleming, and M. Luke, Phys. Rev. D **63**, 014006 (2000); C. W. Bauer, S. Fleming, D. Pirjol, and I. W. Stewart, Phys. Rev. D **63**, 114020 (2001); C. W. Bauer and I. W. Stewart, Phys. Lett. B **516**, 134 (2001); C. W. Bauer, D. Pirjol, and I. W. Stewart, Phys. Rev. D **65**, 054022 (2002).
[10] C. M. Arnesen, Z. Ligeti, I. Z. Rothstein, and I. W. Stewart, Phys. Rev. D **77**, 054006 (2008).
[11] M. Beneke, G. Buchalla, M. Neubert, and C. T. Sachrajda, Phys. Rev. Lett. **83**, 1914 (1999); Nucl. Phys. **B591**, 313 (2000).
[12] M. Beneke, G. Buchalla, M. Neubert, and C. T. Sachrajda, Nucl. Phys. **B606**, 245 (2001); M. Beneke and M. Neubert, Nucl. Phys. **B651**, 225 (2003).
[13] F. Su, Y. D. Yang, G. R. Lu, and H. J. Hao, Eur. Phys. J. C **44**, 243 (2005).
[14] Q. Chang, X. Q. Li, and Y. D. Yang, J. High Energy Phys. 09 (2008) 038.
[15] M. Beneke, J. Rohrer, and D. S. Yang, Nucl. Phys. **B774**, 64 (2007).
[16] H. Y. Cheng and K. C. Yang, Phys. Rev. D **78**, 094001 (2008); **79**, 039903(E) (2009).
[17] H. Y. Cheng and C. K. Chua, Phys. Rev. D **80**, 114026 (2009).
[18] G. Buchalla, A. J. Buras, and M. E. Lautenbacher, Rev. Mod. Phys. **68**, 1125 (1996).
[19] M. Beneke, X. Q. Li, and L. Vernazza, Eur. Phys. J. C **61**, 429 (2009).
[20] F. Su, Y. L. Wu, Y. D. Yang, and C. Zhuang, Eur. Phys. J. C **48**, 401 (2006); Commun. Theor. Phys. **49**, 707 (2008); A. A. Natale and C. M. Zanetti, Int. J. Mod. Phys. A **24**, 4133 (2009); Q. Chang, X. Q. Li, and Y. D. Yang, J. High Energy Phys. 05 (2009) 056; Int. J. Mod. Phys. A **26**, 1273 (2011); Q. Chang and Y. D. Yang, Nucl. Phys. **B852**, 539 (2011).
[21] J. M. Cornwall, Phys. Rev. D **26**, 1453 (1982); J. Papavassiliou and J. M. Cornwall, Phys. Rev. D **44**, 1285 (1991).
[22] LHCb Collaboration, Phys. Lett. B **709**, 50 (2012).
[23] CDF Collaboration, Phys. Rev. Lett. **108**, 211803 (2012).
[24] G. Eilam, M. Ladisa, and Y. D. Yang, Phys. Rev. D **65**, 037504 (2002).
[25] J. Charles, A. Höcker, H. Lacker, S. Laplace, F. R. Le Diberder, J. Malclés, J. Ocariz, M. Pivk, and L. Roos (CKMfitter Group), Eur. Phys. J. C **41**, 1 (2005) (updated results and plots available at http://ckmfitter.in2p3.fr).
[26] K. Nakamura *et al.* (Particle Data Group), J. Phys. G **37**, 075021 (2010).
[27] Tevatron Electroweak Working Group, CDF Collaboration, and D0 Collaboration, arXiv:0808.1089.
[28] Q. Mason, H. D. Trottier, R. Horgan, C. T. H. Davies, and G. P. Lepage (HPQCD Collaboration), Phys. Rev. D **73**, 114501 (2006).
[29] E. Gamiz, C. T. H. Davies, G. P. Lepage, J. Shigemitsu, and M. Wingate (HPQCD Collaboration), Phys. Rev. D **80**, 014503 (2009).
[30] P. Ball and R. Zwicky, Phys. Rev. D **71**, 014015 (2005); **71**, 014029 (2005); Phys. Lett. B **633**, 289 (2006).